羌塘地块西部晚三叠世灰岩古地磁研究及其构造意义

曹勇[1,2)]，孙知明[1)]，李海兵[2)]，叶小舟[1)]，潘家伟[2)]，张蕾[2)]，刘栋梁[2)]，刘晨光[1)]

1）中国地质科学院地质力学研究所，自然资源部古地磁与古构造重建重点实验室，北京，100081；
2）中国地质科学院地质研究所，自然资源部深地动力学重点实验室，北京，100037

内容提要：青藏高原羌塘地块和拉萨地块汇聚—碰撞拼合过程的研究对认识青藏高原中部隆升历史及其动力学过程具有重要的科学意义，而羌塘地块古地磁研究对理解上述问题至关重要。通过对羌塘地块西部改则地区晚三叠世灰岩的系统古地磁测定，获得其高温剩磁分量。但是这一高温剩磁分量未通过褶皱检验，表明为后期重磁化的结果。研究剖面高温特征剩磁平均方向在地理坐标下为 $Dg=349.3°$，$Ig=40.4°$，$\kappa g=45.4$，$\alpha_{95}=6.5°$，相应的古地磁极为76.4°N，311.1°E，$dp/dm=4.7°/7.9°$。这一古地磁极与羌塘地块早白垩世约110～100 Ma的古地磁极在古地磁误差范围内重合，表明其重磁化的时代为早白垩世约110～100 Ma。综合分析羌塘地块和拉萨地块古地磁结果，并结合海相地层、蛇绿岩和洋岛等地质证据，显示班公湖—怒江特提斯洋西段闭合的时间发生在早白垩世晚期约110～100 Ma。改则地区晚三叠世灰岩的早白垩世晚期重磁化作用与羌塘/拉萨地块西部的碰撞密切相关。

关键词：羌塘地块；古地磁；重磁化；羌塘—拉萨地块碰撞；班公湖—怒江洋

青藏高原经历了特提斯体系的长期演化，是地质历史过程中高原上诸地块在不同时期碰撞—拼合至欧亚大陆南缘而形成的(Sengör, 1987; Dewey et al., 1988; Yin An et al., 2000; Metcalfe, 2006, 2013; Xu Zhiqin et al., 2011; Wang Chengshan et al., 2014; Zhu Dicheng et al., 2016)。青藏高原诸地块间如何碰撞—拼合及其持续效应是研究青藏高原形成和演化的重要科学问题(Yin et al., 2000; Metcalfe, 2006, 2013; Xu Zhiqin et al., 2011; Zhu Dicheng et al., 2013; Yan Maodu et al., 2016)。羌塘地块和拉萨地块的碰撞造成了大量的陆内构造缩短，导致青藏高原中部在印度与亚洲大陆碰撞前就可能已有一定的海拔高度(Murphy et al., 1997; Kapp et al., 2005, 2007; Volkmer et al., 2007, 2014)，形成白垩纪时期的青藏高原雏形(Wang Chengshan et al., 2014; Xu Zhiqin et al., 2016)。另外，班公湖—怒江缝合带不仅是一条重要的构造界线，而且是一条重要的成矿带，具有巨大的成矿潜力(Song Yang et al., 2014; Gao Ke et al., 2017; Liu Hong et al., 2017; Tang Juxing et al, 2017; Zheng Youye et al., 2017)。班公湖—怒江缝合带所代表的洋盆的闭合时间是重要的成矿期。因此，羌塘地块和拉萨地块汇聚—碰撞拼合过程(班公湖—怒江特提斯洋演化和闭合过程)的研究不仅对认识青藏高原中部早期隆升历史和动力学过程具有重要的科学意义，而且还可为查明班公湖—怒江成矿带区域成矿规律提供清楚明确的地质构造背景。

前人根据不同研究方法对羌塘地块和拉萨地块汇聚—碰撞过程和班公湖—怒江洋演化及闭合过程进行了深入研究和探讨，并取得了丰富的研究成果，但是至今还存在较大争议。例如，不同学者提出的羌塘地块与拉萨地块碰撞及班公湖—怒江特提斯洋闭合的时代自中—晚侏罗世(Xu Ronghua et al.,

注：本文为国家自然科学基金项目(编号：41672218 和 41672211)、中国地质调查项目(编号：DD20160022-03 和 DD20190059)、中国地质科学院基本科研业务费项目(编号：JYYWF201810)和自然资源部深地动力学重点实验室开放基金项目资助成果。
收稿日期：2019-07-28；改回日期：2019-08-09；网络发表日期：2019-08-23；责任编辑：黄敏。
作者简介：曹勇，男，1989年生。博士，助理研究员。构造地质学专业。Email：geocao@126.com。

引用本文：曹勇，孙知明，李海兵，叶小舟，潘家伟，张蕾，刘栋梁，刘晨光. 羌塘地块西部晚三叠世灰岩古地磁研究及其构造意义. 2019. 地质学报，93(10)：2463～2476，doi：10.19762/j.cnki.dizhixuebao.2019251.
Cao Yong, Sun Zhiming, Li Haibing, Ye Xiaozhou, Pan Jiawei, Zhang Lei, Liu Dongliang, Liu Chenguang. 2019. Paleomagnetic study of the Late Triassic limestones in the western portion of the Qiangtang Block and its tectonic implications. Acta Geologica Sinica, 93(10): 2463～2476.

1985；Dewey et al.，1988；Li Shun et al.，2017；Ma Anlin et al.，2017，2018；Sun Gaoyuan et al.，2019）、早白垩世（Kapp et al.，2005，2007；Mo Xuanxue et al.，2006；Zhu Dicheng et al.，2016；Huang Tongtong et al.，2017；Ma Yiming et al.，2018；Lei Chuanyang et al.，2019）至晚白垩世（Zhang Kaijun et al.，2012；Li Yalin et al.，2013，2015；Liu Deliang et al.，2014；Liu Weiliang et al.，2014；Fan Jianjun et al.，2014，2015；Wang Baodi et al.，2016；Chen Weiyan et al.，2018）不等。羌塘地块与拉萨地块碰撞为近南北向的陆－陆碰撞，那么定量约束两块体碰撞时和碰撞前古纬度位置对认识羌塘地块与拉萨地块汇聚－碰撞过程和班公湖－怒江特提斯洋的演化及闭合过程等科学问题有重要意义。古地磁学能定量地约束板块的古纬度，在地块古地理位置重建和地块运动学的研究上具有独特的优势，是制约板块间相互作用最理想方法之一。但是，目前羌塘地块古地磁学研究相对比较薄弱，尤其是中生代可靠的古地磁数据非常有限。另外，现有可靠的古地磁结果主要来自羌塘地块中－东部地区（Cheng Xin et al.，2012；Song Chunyan et al.，2012；Ren Haidong et al.，2013；Song Peiping et al.，2015，2017；Tong Yabo et al.，2015；Yan Maodu et al.，2016；Ran Bo et al.，2017；Meng Jun et al.，2018；Cao Yong et al.，2019；Ma Yiming et al.，2019）（图 1），而由于印度与亚洲大陆碰撞以及青藏高原中部大量走滑断裂作用的影响，白垩纪以来青藏高原中部不同地区之间都存在不同的局部水平旋转作用，就导致羌塘地块中－东部地区的古地磁极数据很难用来约束羌塘地块西部的古地理位置及其运动过程。本文选择羌塘地块西部改则地区晚三叠世灰岩开展古地磁研究，以期为羌塘地块与拉萨地块汇聚－碰撞过程和班公湖－怒江特提斯洋演化及闭合过程提供古地磁定量约束。

1　地质背景及样品采集

青藏高原南起喜马拉雅山脉南缘，北至阿尔金和祁连山北缘，西临帕米尔高原和喀喇昆仑山脉，东接四川盆地。青藏高原可根据多条缝合带划分成多个不同块体（图 1），从南至北依次为喜马拉雅地块、拉萨地块、羌塘地块、松潘－甘孜－可可西里地块、昆仑地块－柴达木地块和祁连地块。羌塘地块位于青藏高原腹地，东西长约 1200 km，中部宽约 500～

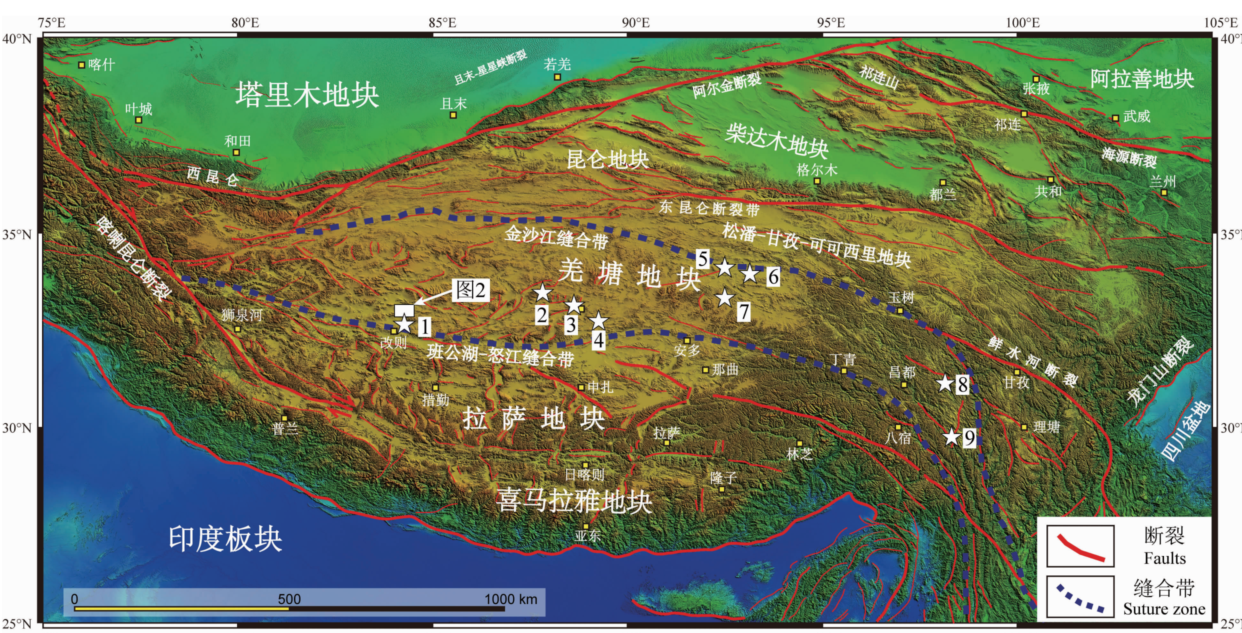

图 1　青藏高原及其周缘构造简图

Fig. 1　Schematic tectonic map of the Tibetan Plateau and the adjacent region

图中五角星代表现有羌塘地块古地磁结果研究位置分布（the star represent the paleomagnetic research location in Fig. 1）：1—Chen Weiwei et al.，2017；2—Song Chunyan et al，2012；3—Meng Jun et al.，2018；4—Cao Yong et al.，2019；5—Song Peiping et al.，2015，2017；Ma Yiming et al.，2019；6—Halim et al.，1998；7—Cheng Xin et al.，2012；Ren Haidong et al.，2013；Yan Maodu et al.，2016；Ran Bo et al.，2017；8—Tong Yabo et al.，2017；9—Huang Kainian et al.，1992；Tong Yobo et al.，2015

600 km，西部和东部宽度小于 150 km（Yin et al.，2000）。羌塘地块南以班公湖—怒江缝合带为界与拉萨地块相邻，北以金沙江缝合带为界与松潘—甘孜—可可西里地块相邻（图 1）。近年来，地质学家们在羌塘地块中西部变质杂岩带中，沿龙木错—双湖一线发现古特提斯阶段的蛇绿混杂岩、榴辉岩和蓝片岩的各种组分，且发现该带两侧的古生物面貌和沉积地层完全不同（Xu Zhiqin et al.，2013）。Li Cai（1987）曾提出该带为一条北西西—南东东向的板块缝合带（龙木错—双湖—澜沧江板块缝合带），并提出该缝合带为冈瓦纳大陆的北界的观点。许多学者根据龙木错—双湖—澜沧江板块缝合带的发现将羌塘地块划分为南羌塘地块和北羌塘地块（Li Cai et al.，2008，2009；Peng Touping et al.，2015），也有学者称之为西羌塘和东羌塘（Zhang Kaijun et al.，2012；Zhu Dicheng et al.，2013，2016）。

本次研究区位于羌塘地块西部改则县城东北约 90 km 处玛日玛地区，在班公湖—怒江缝合带北侧，龙木错—双湖缝合带以南，构造上属于南羌塘地块（图 1）。区内出露的地层主要是三叠系地层，侏罗系、古近系和新近系地层零星出露（图 2a）。上三叠统日干配错组（T_3r）地层岩石组合以微晶灰岩和鲕粒灰岩为主，产双壳类和珊瑚类等化石（Geological Survey of Tibet Autonomous Region，2006）。下—中侏罗统色哇组（$J_{1-2}s$）地层岩石总体以泥质岩为主，产珊瑚化石（Geological Survey of Tibet Autonomous Region，2006），区内与下伏日干配错组地层呈断层接触关系。纳丁错组地层岩性以中—基性火山岩为主，区内与日干配错组以角度不整合接触，研究显示研究区内纳丁错组火山岩的时代为～110 Ma（Kapp et al.，2005；Chang Qingsong et al.，2011）。新近系康托组（Nk）岩石以砾岩夹砂岩为主，区内与日干配错组和色哇组以角度不整合接触。区内东部出露燕山晚期花岗闪长岩（$\gamma\delta K_1$）。Geological Survey of Tibet Autonomous Region（2006）曾在研究区内对日干配错组地层进行了实测地层剖面，实测剖面显示日干配错组岩性以微晶灰岩和鲕粒灰岩为主，其间不同程度夹有角砾状灰岩、砂屑灰岩、泥灰岩、粒屑灰岩、藻灰岩、介屑灰岩。在改则其他区域的日干配错组地层中发现生物礁灰岩为海绵礁和珊瑚礁，鉴定结果为晚三叠世（Geological Survey of Tibet Autonomous Region，2006）。

本次古地磁采样工作在玛日玛村至扎美仁村公路沿线一带日干配错组地层内开展。采样剖面地层出露较好，岩石新鲜，地层产状清晰（图 2b～2e），共采集了 23 个古地磁采点约 224 块岩心样品。剖面北部采点 MT1～MT3 所在地层朝 SSW 倾，采点 MT4～MT10 所在地层朝 NNE 倾，采点 MT13～MT20 所在地层朝 SSE 倾，采样剖面地层总体上地层倾向方向变化较大。另外，采样剖面地层倾角也变化较大，倾角从～40°至近直立。

2　古地磁测试与分析

全部样品在室内加工成标准古地磁样品，并利用 TD-48 大型热退磁炉进行系统热退磁处理。热退磁温度在低温段间隔为 50～60 ℃，高温段间隔为 20～30 ℃。样品的剩磁测量利用 2G-755R 超导磁力仪进行。为确定岩石中样品的主要载磁矿物，对代表样品进行了三轴等温剩磁热退磁实验，测试仪器为 JR-6A 旋转磁力仪。以上测试均在自然资源部古地磁与古构造重建重点实验室磁屏蔽屋内进行。磁屏蔽屋内的磁场＜300 nT，排除了外界磁场对样品测试数据的影响。样品的退磁结果分析利用主向量法（Kirschvink，1980），最后以采样点为单位进行 Fisher 统计分析（Fisher，1953）。

2.1　三轴等温剩磁热退磁结果

对日干配错组灰岩代表样品的 Z 轴、Y 轴和 X 轴方向依次施加 2.5 T、0.4 T 和 0.12 T 磁场，然后对样品进行系统热退磁实验。三轴等温剩磁热退磁实验结果显示，样品 MT3-2 和 MT11-5A 的三中磁性成分的剩磁强度均在～680 ℃时衰减至接近为零（图 3a，3c）；样品 MT8-6A 和 MT20-4 的硬磁成分的剩磁强度在～680 ℃时衰减至接近为零，而中间磁成分和软磁成分的剩磁强度在～580 ℃时接近为零（图 3b，3d）。以上结果表明日干配错组样品中的主要载磁矿物为赤铁矿和磁铁矿。

2.2　系统热退磁结果

日干配错组灰岩样品系统热退磁结果显示大多数样品只存在单一剩磁分量（图 4a，4d，4g，4h）。样品在 180 ℃至 580 ℃或 680 ℃温度段之间可分离出一组高温剩磁分量。日干配错灰岩古地磁样品数据经分析后，共获得了 12 个采点的高温特征剩磁分量（表 1）。12 个采样点高温特征剩磁分量的平均磁化方向为：$Dg=349.3°$，$Ig=40.4°$，$\kappa g=45.4$，$\alpha_{95}=6.5°$（地理坐标下）；$Ds=247.0°$，$Is=83.6°$，$\kappa s=2.2$，$\alpha_{95}=39.0°$（层面坐标下）（表 1，图 5）。

日干配错组样品高温特征剩磁分量经产状校正后变得更加分散（$kg/ks=20.6$）（图 5）。另外，古地

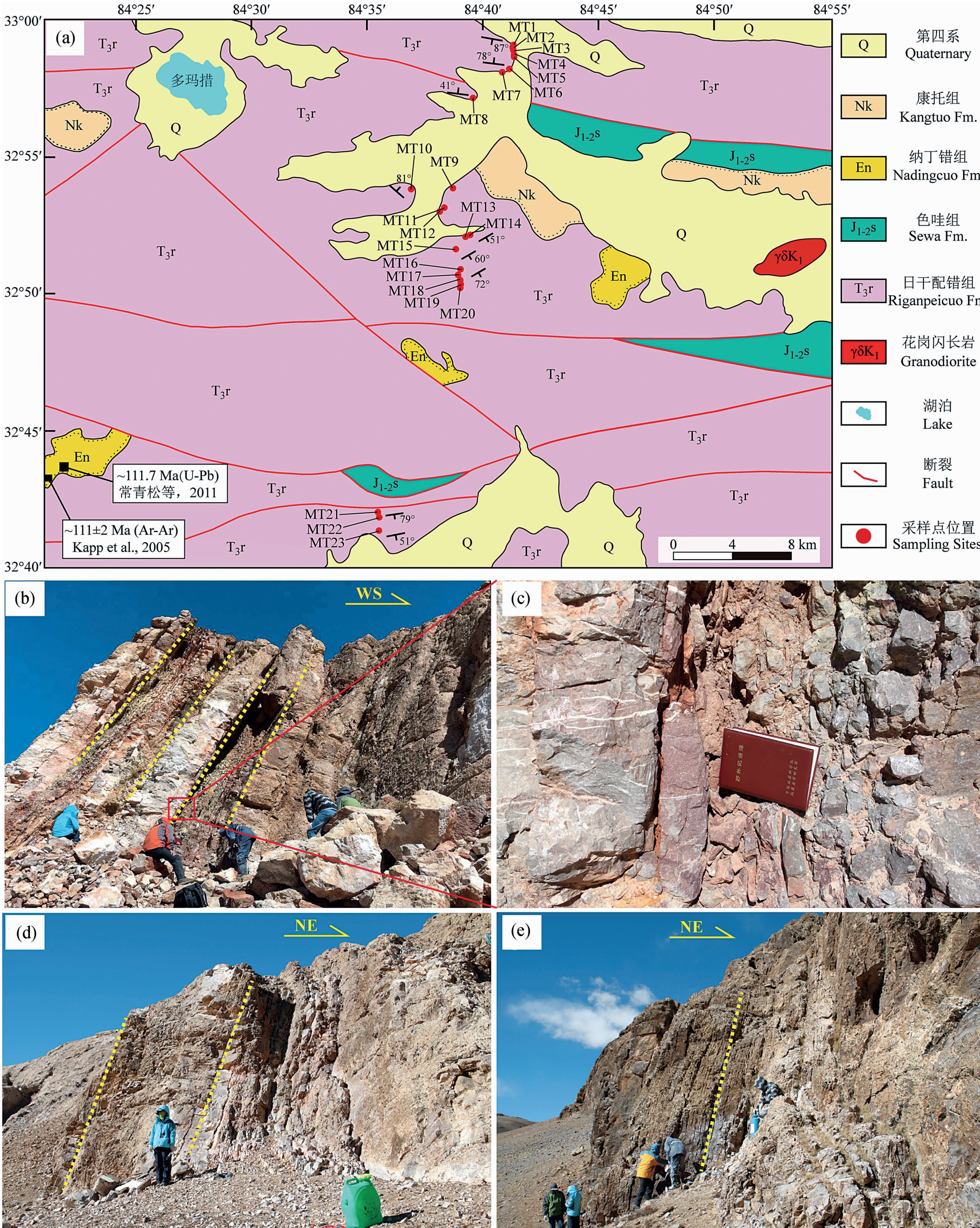

图 2 羌塘地块西部玛日玛地区地质简图(a)和上三叠统日干配错组地层野外露头及采样照片(b～e)

Fig. 2 Simplified geological map of the Marima area in the western portion of the Qiangtang block (a) and photographs showing field outcrops and sampling sites of the Upper Triassic Riganpeicuo Formation (b～e)

磁数据未通过褶皱检验($\xi_{in\text{-}situ}=2.884<\xi_c=4.036<\xi_{tilt\text{-}corrected}=8.47$ 在 95%置信区间为负褶皱检验；$\xi_{in\text{-}situ}=5.308<\xi_c=5.624<\xi_{tilt\text{-}corrected}=11.64$ 在 99%置信区间也为负褶皱检验)(McFadden, 1990)。高温特征剩磁分量的逐步褶皱展平检验(Watson et al., 1993)结果显示 Fisher 统计精度参数 k 的极大值出现在−1.8%展平状态，表明日干配错地层单元的特征剩磁是在褶皱变形之后获得的。以上结果显示本次研究从日干配错组地层中获得的晚三叠世古地磁数据为后期重磁化结果。

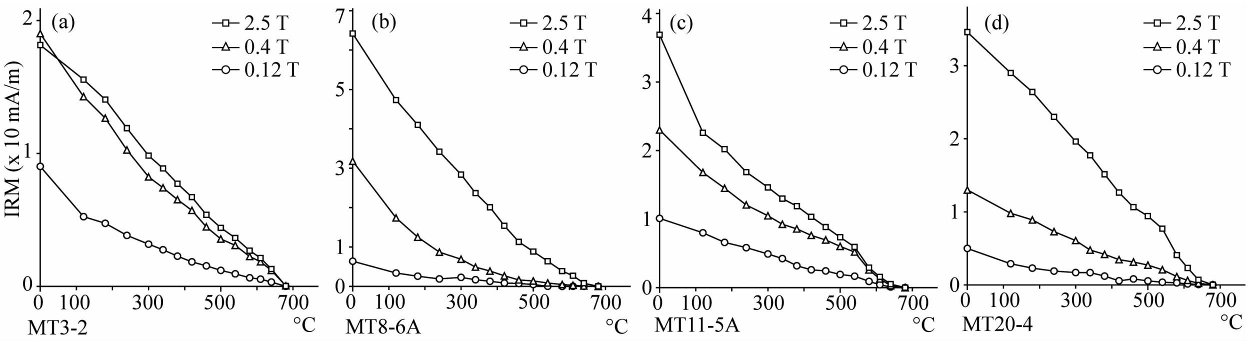

图 3　羌塘地块西部上三叠统日干配错组岩石代表样品三轴等温剩磁热退磁结果图

Fig. 3　Thermal demagnetization of three-component isothermal remanent magnetization for representative samples from the Upper Triassic Riganpeicuo Formation in the western portion of the Qiangtang block

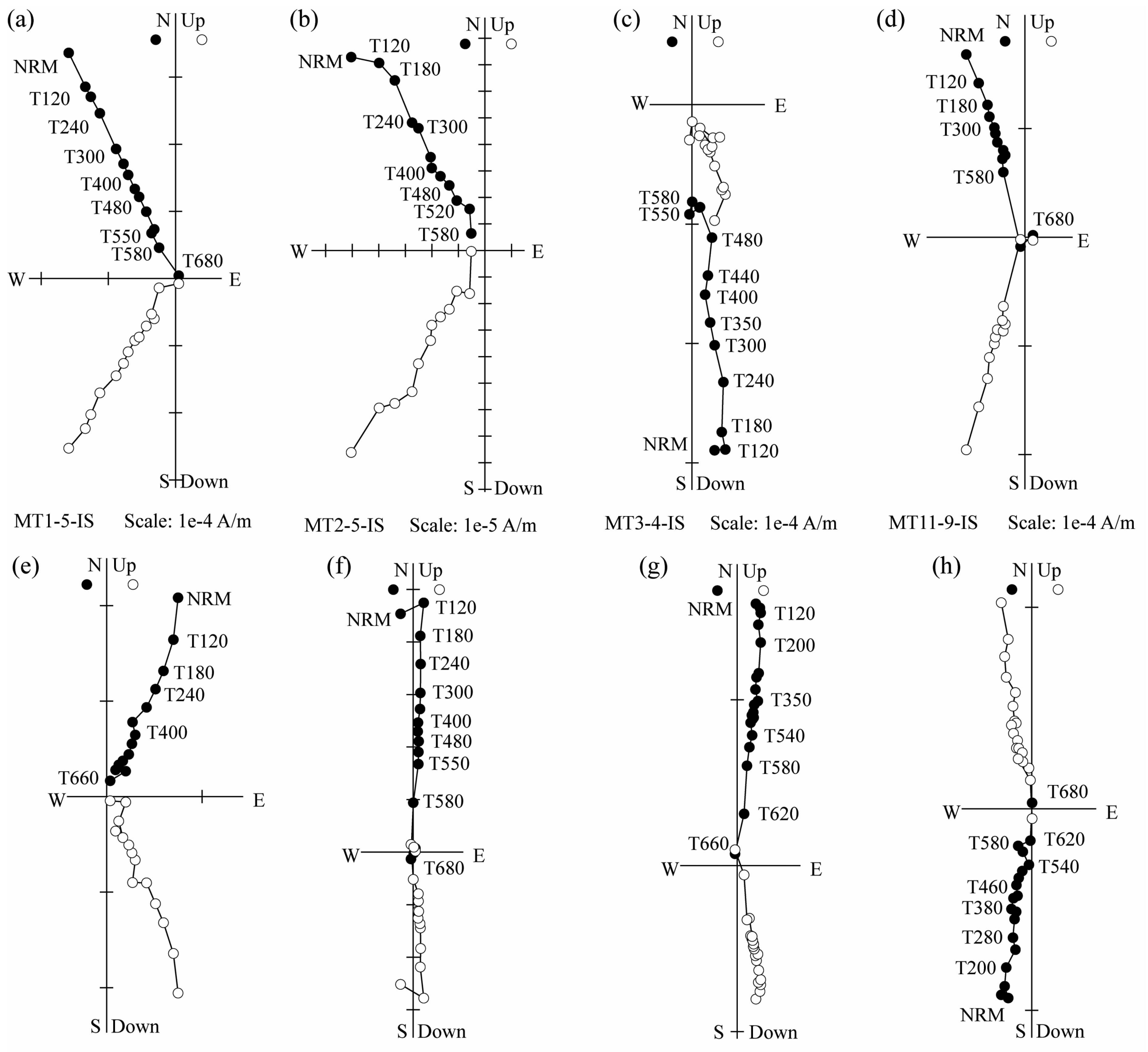

图 4　羌塘地块西部上三叠统日干配错组岩石代表样品 Z 矢量图(地理坐标下)

Fig. 4　Orthogonal vector diagrams of representative samples from the Upper Triassic Riganpeicuo Formation in the western portion of the Qiangtang block (in situ coordinates)

实心圆圈和空心圆圈分别代表剩磁方向在水平面和铅垂面上的投影

The solid and open circles represent vectors endpoints projected onto horizontal and vertical planes, respectively

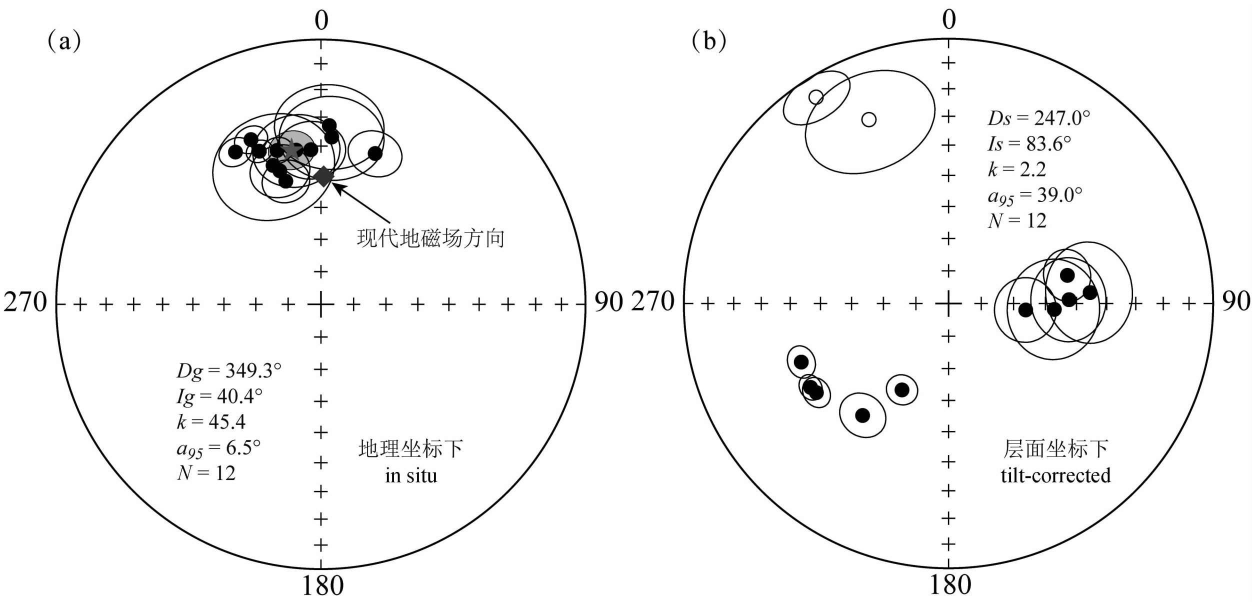

图 5 羌塘地块西部上三叠统日干配错组岩石样品高温特征剩磁分量地理坐标下(a)和层面坐标下(b)赤平投影图

Fig. 5 In situ (a) and tilt-corrected (b) equal-area projections of site-mean directions from the Upper Triassic Rigampeicuo Formation in the western portion of the Qiangtang block

表 1 羌塘地块西部上三叠统日干配错组岩石样品高温特征剩磁分量结果统计表

Table 1 Site-mean paleomagnetic directions of the high-temperature components from the Upper Triassic Riganpeicuo Formation in the western portion of the Qiangtang block

采点	走向/倾向	n/N	Dg (°)	Ig (°)	Ds (°)	Is (°)	κ	α_{95} (°)
MT1	110/87	7/11	337.0	32.9	248.3	39.9	172.2	4.6
MT2	108/88	9/10	338.1	37.7	238.7	38.9	190.3	3.7
MT3	110/89	7/8	344.1	39.4	236.0	39.6	190.8	4.4
MT9	205/65	4/6	342.9	46.2	327.3	−8.2	114.0	8.6
MT11	230/72	5/9	341.0	43.8	336.6	−25.3	20.1	17.5
MT13	60/51	10/10	19.8	39.3	76.7	51.9	41.8	7.6
MT15	60/60	6/10	356.3	41.1	94.8	66.1	48.6	9.7
MT17	49/74	8/10	3.7	36.8	85.6	45.4	15.8	14.4
MT18	45/71	9/10	350.9	40.7	88.2	52.4	18.8	12.2
MT19	60/72	6/8	2.7	32.9	93.2	57.1	21.4	14.8
MT21	82/79	6/9	330.7	34.4	208.3	59.6	201.4	4.7
MT22	102/78	4/9	344.1	50.0	217.5	45.7	177.5	6.9
Mean		12(81)	349.3	40.4	—	—	45.4	6.5
			—	—	247.0	83.6	2.2	39.0

注:n/N 为参加统计/剩磁测量样品数;Dg,Ig(Ds,Is)分别为地理坐标下(层面坐标下)特征剩磁的偏角和倾角;κ,α_{95} 分别为 Fisher 统计精度参数和平均方向的 95%置信圆锥半顶角。

3 讨论

3.1 重磁化时代

Van der Voo (1990)提出了 7 条古地磁数据可靠性判别标准,我们在此基础上重点考察羌塘地块白垩纪以来的古地磁结果是否通过稳定性检验和是否经过构造校正,从而筛选出可靠地古地磁数据(表 2)。值得注意的是,Chen Weiwei et al. (2017)发表的早白垩世 110~100 Ma 的古地磁结果中 GZ35-36、GZ37、GZ38 和 GZ39-41 四个点的古地磁结果明显偏离其他 10 个采点的结果(见 Chen Weiwei et al., 2017 图 8f),因此这 4 个采点的结果不再进行分析。其余 10 个采点的古地磁结果的平均方向为 Ds/Is=346.9°/42.0°,α_{95}=5.1°;相应的古地磁极位置为 75.8 °N/321.9 °E,dp/dm=3.8°/6.3°。这一古地磁结果也通过褶皱检验($\xi_{\text{in-situ}}=6.327>\xi_c=3.685>\xi_{\text{tilt-corrected}}=3.492$ 在 95%置信区间为正褶皱检验;$\xi_{\text{in-situ}}=6.327>\xi_c=5.12>\xi_{\text{tilt-corrected}}=3.492$ 在 99%置信区间也为正褶皱检验)。此外,Meng Jun et al. (2018)对羌塘地块双湖县城附近上白垩统阿布山组砂岩开展了古地磁学研究,从 70 余块样品中获得了相应的中温分量和高温分量。Meng Jun et al. (2018)将中温分量和高温分量分别进行 E/I 矫正分析。中温分量平均磁倾角为 46.1° ± 2.9°,中温分量 E/I 矫正结果平均倾角为 48.8°(置信范围为 45.1° ~ 59.6°),表明其中温分量结果未受到明显的磁倾角浅化作用的影响。高温分量平均磁倾角为 37.2° ± 3.7°,高温分量 E/I 矫正结果平均倾角为 42.8°(置信范围为 36.3° ~ 51.2°)。Meng Jun et al. (2018)认为其研究结果高温分量磁倾角发生

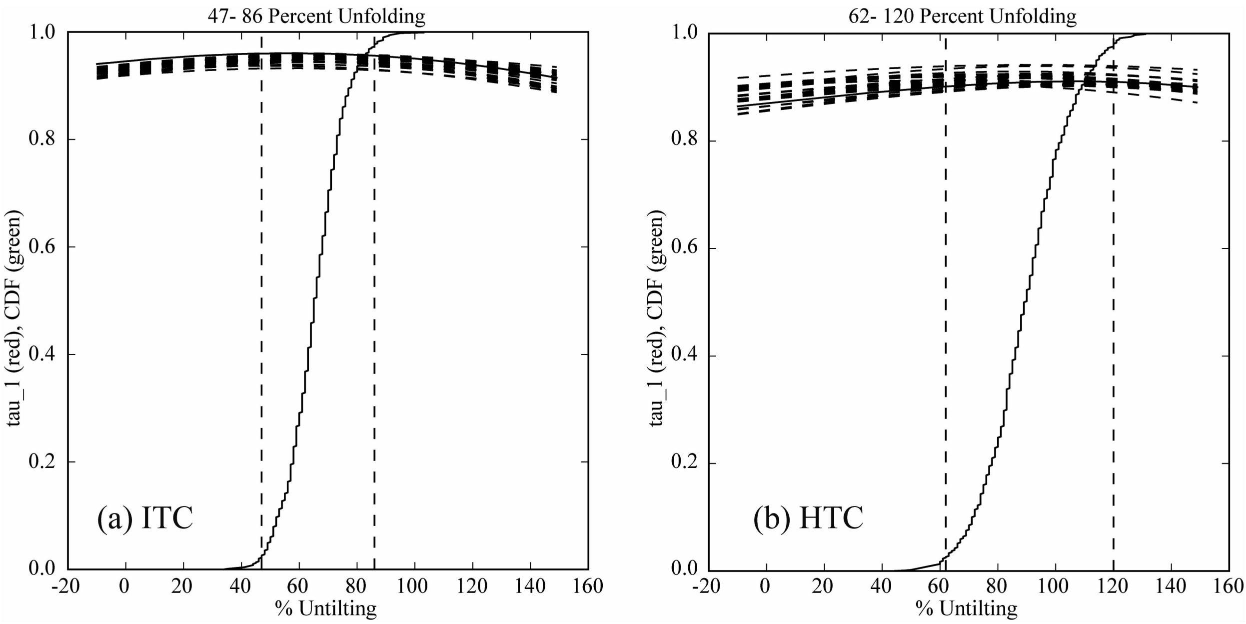

图 6　Meng Jun et al.（2018）研究中温分量(a)和高温分量(b)褶皱检验结果图

Fig. 6　Nonparametric fold tests of the Intermediate Temperature Component (ITC) and High Temperature Component (HTC) directions from Meng Jun et al. (2018)

了浅化现象，因此其用中温分量结果来限定羌塘地块晚白垩世的古纬度。但是其高温分量的原始平均磁倾角(I=37.2°±3.7°)却在 E/I 矫正结果的磁倾角置信范围内，并不能说明其研究地层磁倾角发生了明显浅化现象。另外，我们对 Meng Jun et al.(2018)所发表的结果进行基于样品数据的褶皱检验(Tauxe et al., 1994)。褶皱检验结果显示其中温分量很可能在褶皱形成过程中获得的(图 6a)，而其高温分量则可能是在褶皱前获得的(图 6b)。因此，我们参考 Meng Jun et al.(2018)所报道的羌塘地块晚白垩世古地磁研究的高温特征剩磁分量数据结果来进行进一步讨论。

本次研究从羌塘地块西部改则地区上三叠统日干配错组灰岩中获得磁化方向为：Dg=349.3°，Ig=40.4°，κg=45.4，α_{95}=6.5°，相应的古地磁极为76.4 °N，311.1 °E，dp/dm=4.7°/7.9°。与羌塘地块白垩纪以来可靠的古地磁极数据对比，显示本次研究获得的古地磁极与羌塘地块晚白垩世古地磁极(Huang Kainian et al., 1992; Tong Yabo et al., 2015; Chen Weiwei et al., 2017; Meng Jun et al.,

表 2　羌塘地块白垩纪—新近纪古地磁极统计表

Table 2　Summary of the Cretaceous-Neogene paleomagnetic results from the Qiangtang block

SLat. (°N)	SLon. (°E)	时代 (Ma)	N/n	Plat. (°N)	Plon. (°E)	A_{95} (dp/dm) (°)	检验	古纬度 (°N)	参考文献
地块西部									
34.5	92.7	E	7/31	72.2	242.1	7.7	F,R	15.8 ± 9.4	Halim et al., 1998
33.2	88.7	K_2	9/71	29.2	171.8	2.5/4.3	F	16.9 ± 3.9	Meng Jun et al., 2018
32.5	84.3	K_2	22/174	45.4	348.1	3.1	F	18.8 ± 3.6	Chen Weiwei et al., 2017
32.5	84.3	110～100	10/57	75.8	321.9	3.8/6.3	F	24.3 ± 5.1	ChenWeiwei et al., 2017
32.9	84.7	110～100	12/81	76.4	311.1	4.7/7.9	—	22.8± 6.5	本次研究
32.9	83.5	120～115	16/127	37.9	162.2	5.1	—	27.8 ± 4.9	Cao Yong, 2018
地块东部									
31.0	98.2	E_2	43/352	57.9	192.1	2.9	F,R	18.4 ± 3.4	Tong Yabo et al., 2017
29.7	98.4	K_2	17/186	47.0	165.1	6.7/9.3	F,R	28.8 ± 7.5	Tong Yabo et al., 2015
29.7	98.7	K_2	11/64	56.7	172.7	10.6	F	27.4 ± 10.4	Huang Kainian et al., 1992
29.7	98.4	K_1	12/56	40.6	170.5	13.0	F	22.9±13.9	Huang Kainian et al., 1992

注：Slat. 和 Slon. 分别为采样点的纬度和经度；N/n 为采点数/样品数；Plat. 和 Plon. 分别为古地磁极的经度和纬度；A_{95} 为为古地磁极的95%置信圆锥半顶角；dp/dm 为 95% 置信椭圆半长轴与半短轴；F 代表通过褶皱检验；R 代表通过倒转检验；古纬度是以改则为参考点(32.5°N / 84 °E)计算。

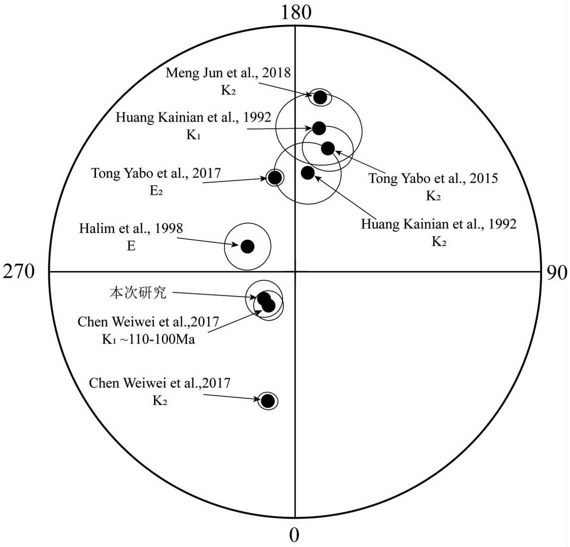

图 7 羌塘地块白垩纪—新近纪古地磁极赤平投影图

Fig. 7 Equal-area projection of the Cretaceous-Neogene paleomagnetic poles of the Qiangtang block

2018)和古近纪—新近纪古地磁极(Halim et al.，1998；Tong Yabo et al.，2017)均存在较大差异(图7)。另外，本次研究从日干配错组灰岩获得的高温剩磁方向(地理坐标下：D/I=349.3°/40.4°)也与参考点现代地磁场的方向(D/I=1.3°/50.2°)存在差异(图5)。而本次研究获得的古地磁极与 Chen Weiwei et al. (2017)从羌塘地块改则地区早白垩世(110～100 Ma)火山岩中获得的古地磁极重叠(图7)。以上分析表明羌塘地块西部改则地区晚三叠世灰岩的重磁化时代应为早白垩世 110～100 Ma。

3.2 构造意义

本次研究从晚三叠世灰岩获得的重磁化结果与 Chen Weiwei et al. (2017)从早白垩世(110～100 Ma)火山岩中获得的古地磁结果一致，综合古地磁结果表明羌塘地块西部南缘在约 110～100 Ma 期间位于 23.3 ± 4.0 °N。拉萨地块西部白垩纪古地磁研究结果见表 3，利用小圆弧拟合法对 Chen Weiwei et al. (2012)、Ma Yiming et al. (2014)和 Bian Weiwei et al. (2017)从拉萨地块西部早白垩世火山岩中获得的高质量古地磁极以改则为参考点(32.5 °N / 84 °E)进行小圆弧拟合，获得拉萨地块西部北缘早白垩世的古纬度为 20.1 ± 2.4 °N(图8a)。对比羌塘地块和拉萨地块西部早白垩世古纬度显示两地块西部地区在早白垩世晚期 110～100 Ma 的古纬度差为 3.2° ± 3.1°，显示在古地磁误差范围内无明显差别。另外，拉萨地块西部晚白垩世古地磁极分布在以改则参考点为圆心以 74.2° ± 2.7°为半径的圆弧上，对比羌塘地块晚白垩世古地磁结果显示两地块在晚白垩世时期古纬度已经重叠(图 8b)。而根据改则西北部早白垩世火山岩中获得的古地磁结果显示羌塘地块西部南缘在 120～115 Ma 时期的古纬度为 27.8 ± 4.9 °N(Cao Yong，2018)，表明在 120～115 Ma 羌塘地块和拉萨地块西部之间还存在 7.2° ± 5.5°的古纬度差。

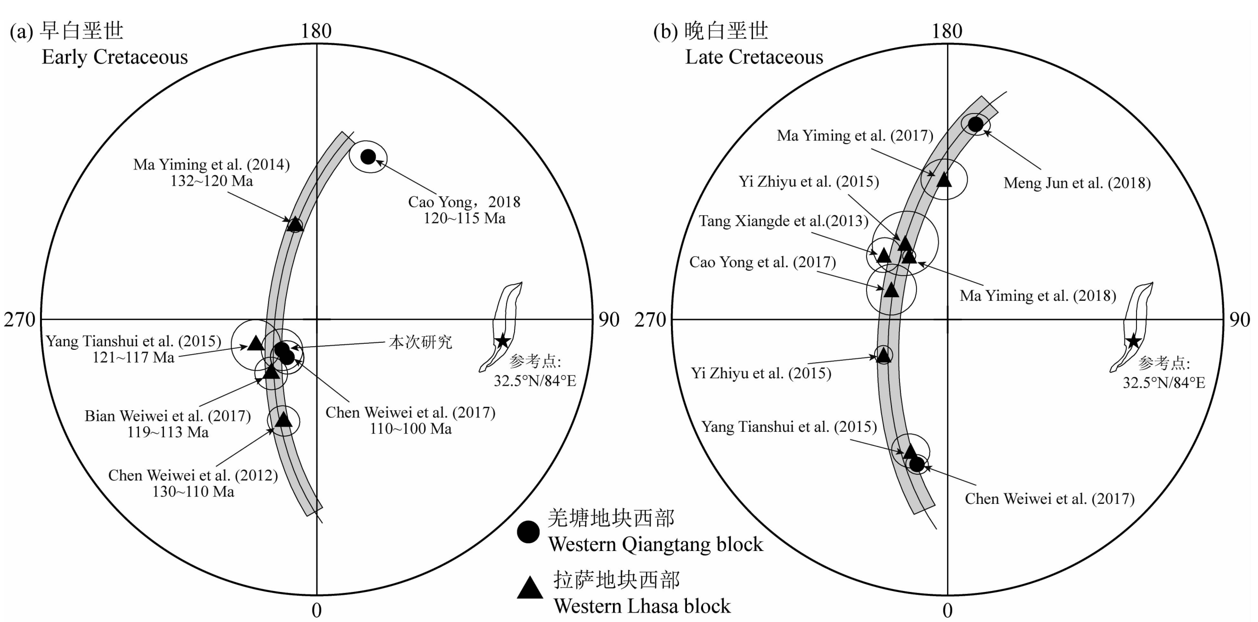

图 8 羌塘地块和拉萨地块西部早白垩世(a)和晚白垩世(b)古地磁极赤平投影图

Fig. 8 Equal-area projection showing the available Early (a) and Late (b) Cretaceous paleomagnetic poles obtained from the western portion of the Qiangtang and Lhasa blocks

表 3　拉萨地块西部白垩纪古地磁极统计表

Table 3　Summary of the Cretaceous paleomagnetic poles from the western portion of the Lhasa block

SLat. (°N)	SLon. (°E)	时代(Ma)	N/n	Plat. (°N)	Plon. (°E)	$A_{95}(dp/dm)$(°)	古纬度(°N)	参考文献
32.6	80.2	～69	44/306	47.8	181.4	6.4	19.0 ± 7.4	Ma Yiming et al., 2017
32.4	80.1	～92	10/78	64.1	209.0	9.6	15.8 ± 11.7	Yi Zhiyu et al., 2015
31.6	82.2	～80	15/136	68.4	298.8	2.7	14.2 ± 3.4	Yi Zhiyu et al., 2015
31.2	84.7	K_2	33/291	49.0	344.3	5.3	18.2 ± 6.2	Yang Tianshui et al., 2015
30.9	85.1	99～93	10/82	63.1	224.6	5.1	10.6 ± 6.7	Tang Xiangde et al., 2013
31.8	87.2	K_2	8/59	71.2	241.9	5.5/10.0	14.9 ± 8.8	Cao Yong et al., 2017
32.2	80.8	K_2	38/274	68.0	211.1	1.9	17.9 ± 2.2	Ma Yiming et al., 2018
32.2	80.4	116～113	19/205	69.1	319.8	4.8	19.4 ± 5.5	Bian Weiwei et al., 2017
31.1	81.4	121～117	12/116	70.5	292.9	7.4	15.1 ± 9.1	Yang Tianshui et al., 2015
32.3	82.6	132～120	51/444	61.4	192.9	2.1	19.9 ± 2.4	Ma Yiming et al., 2014
31.3	85.1	130～110	18/162	58.2	341.9	4.6	21.3 ± 5.1	Chen Weiwei et al., 2012

注:Slat. 和 Slon. 分别为采样点的纬度和经度;N/n 为采点数/样品数;Plat. 和 Plon. 分别为古地磁极的经度和纬度;A_{95} 为为古地磁极的 95%置信圆锥半顶角;dp/dm 为 95% 置信椭圆半长轴与半短轴;古纬度是以改则为参考点(32.5°N / 84 °E)计算。

前人根据地质资料对羌塘地块和拉萨地块碰撞和班公湖—怒江洋闭合时限的问题进行了深入探讨,虽然有些学者认为羌塘地块和拉萨地块碰撞及班公湖—怒江洋闭合的时限为中侏罗—早白垩世早期(Xu Ronghua et al., 1985; Dewey et al., 1988; Zhu Dicheng et al., 2016; Huang Tongtong et al., 2017; Li Shun et al., 2017; Ma Anlin et al., 2017, 2018; Ma Yiming et al., 2018; Sun Gaoyuan et al., 2019)。但是本文通过对羌塘地块和拉萨地块西部白垩纪古地磁数据的综合分析,显示两地块西部在～115 Ma 时还存在 7.2° ± 5.5°的古纬度差,表明班公湖—怒江特提斯洋西部在早白垩世早期并未闭合。而早白垩世晚期 110～100 Ma 时期羌塘地块和拉萨地块西部的古纬度在误差范围内一致,且晚白垩世时期两地块西部的古纬度已经重叠。以上证据表明羌塘地块和拉萨地块西部发生碰撞以及班公湖—怒江特提斯洋的最终闭合时间在约 110～100 Ma。

班公湖—怒江缝合带西段最高海相地层、蛇绿岩和洋岛等地质证据也支持这一观点。首先,羌塘地块西部存在早白垩世早期的海相地层(Bi Zhiwei et al., 2018; Chen Weiyan et al., 2018; Meng Jun et al., 2018)。Bi Zhiwei et al. (2018)在羌塘地块西南缘发现一套晚侏罗世—早白垩世的海相地层,并获得了该套地层中发育的玄武岩夹层的年龄为 118.3 ± 2.1 Ma。最高海相地层证据表明班公湖—怒江特提斯洋西段在早白垩世早期尚未闭合。其次,班公湖—怒江缝合带西段分布有大量早白垩世蛇绿岩。班公湖—怒江缝合带西段中仓蛇绿岩(114.3 ± 1.4 Ma; Xu Mengjing et al., 2014)、康穷蛇绿岩(114.6 ± 3.7; Xu Wei et al., 2015)、洞措蛇绿岩(～132 ± 3 Ma; Bao Peisheng et al., 2007)和革吉蛇绿岩(126.6 ± 10.2 Ma; Zhang Kaijun et al., 2014)的年代均为早白垩世早期,揭示班公湖—怒江缝合带西段在早白垩世早期尚处于洋盆的形成和发展阶段。另外,Baxter et al. (2009)根据班公湖—怒江缝合带西段拉果措蛇绿岩带中放射虫化石的发现揭示青藏高原中部的深海环境可能一直持续到早白垩世 131～121 Ma,并表明班公湖—怒江洋盆闭合发生在早白垩世晚期。最后,班公湖—怒江缝合带西部分布有早白垩世中期洋岛岩石组合(Fan Jianjun et al., 2014, 2015)。Fan Jianjun et al. (2014, 2015)对班公湖—怒江缝合带西部改则地区仲岗洋岛岩石的地球化学和地质年代学研究表明其形成于以洋壳为基底的大洋洋岛环境,形成时代为早侏罗至早白垩世早期(185～116 Ma)。这表明班公湖—怒江特提斯洋在早白垩世早期仍未闭合(Fan Jianjun et al., 2018)。

造山带内碳酸盐岩易于受到后期重磁化作用的影响(Huang Wentao et al., 2017a, 2017b, 2019),而其重磁化与块体间相互碰撞作用有关(Huang Wentao et al., 2019)。块体的碰撞的强烈作用可能会导致岩石中黄铁矿和磁铁矿氧化生成赤铁矿,从而产生重磁化作用(Huang Wentao et al., 2019)。羌塘地块与拉萨地块碰撞造成了强烈的构造变形和地壳短缩(Murphy et al., 1997; Kapp et al., 2005; Volkmer et al., 2007)。根据前文分析显示羌塘地块与拉萨地块西部碰撞发生在早白垩世晚期,与本次研究获得的羌塘地块西部晚三叠世灰岩的重磁化时代非常一致。因此,我们认为羌塘地块西部晚三叠世灰岩的重磁化作用与羌塘/拉萨地块的碰撞密切相关。羌塘地块西部晚三叠世灰岩在

早白垩世晚期发生重磁化作用也是羌塘地块与拉萨地块西部碰撞的响应。

4 结论

(1)本次研究从羌塘地块西部改则地区晚三叠世灰岩中获得的其特征剩磁分量未通过褶皱检验,表明为后期重磁化的结果。研究剖面高温特征剩磁平均方向在地理坐标下平均方向为 $Dg=349.3°$,$Ig=40.4°$,$\kappa g=45.4$,$\alpha_{95}=6.5°$,相应的古地磁极为 76.4 °N,311.1 °E,$dp/dm=4.7°/7.9°$。这一古地磁极与羌塘地块早白垩世约 110～100 Ma 的古地磁极重叠,由此确认本次研究地层重磁化的时代为早白垩世 110～100 Ma。

(2)结合羌塘地块现有可靠的古地磁结果表明羌塘地块西部南缘在约 110～100 Ma 期间位于 23.3 ± 4.0 °N 的古纬度位置。对比拉萨地块西部白垩纪古地磁数据并结合海相地层、蛇绿岩和洋岛等地质证据,提出羌塘地块和拉萨地块西部碰撞以及班公湖—怒江特提斯洋西段闭合的时间在早白垩世晚期约 110～100 Ma。

(3)羌塘地块西部改则地区晚三叠世灰岩的早白垩世晚期重磁化作用与羌塘/拉萨地块西部碰撞密切相关。

References

Bao Peisheng, Xiao Xuchang, Su Li, Wang Jun. 2007. Petrological, geochemical and chronological constraints for the tectonic setting of the Dongco ophiolite in Tibet. Science in China Series D: Earth Sciences, 50: 660～671.

Baxter A T, Aitchison J C, Zyabrev S V. 2009. Radiolarian age constraints on Mesotethyan ocean evolution, and their implications for development of the Bangong-Nujiang suture, Tibet. Journal of the Geological Society, London, 166: 689～694.

Bi Zhiwei, Li Zhimin, Li Qiang, Wang Yankai, Sun Xiao, Zhang Tao. 2018. The discovery of the Upper Jurassic to Lower Cretaceous marine strata on the southwestern margin of the Qiangtang block. Sedimentary Geology and Tethyan Geology, 38(1): 1～10. (in Chinese with English abstract).

Bian Weiei, Yang Tianshui, Ma Yiming, Jin Jingjie, Gao Feng, Zhang Shihong, Wu Huaichun, Li Haiyan. 2017. New Early Cretaceous palaeomagnetic and geochronological results from the far western Lhasa terrane: Contributions to the Lhasa-Qiangtang collision. Scientific Reports, 7: 16216.

Cao Yong, Sun Zhiming, Liu Dongliang, Zhang Lei, Ye Xiaozhou, Zheng Yong, He Xiangli. 2017. Late Cretaceous paleomagnetic results in the Nyima area from the northern margin of the Lhasa block and its tectonic implications. Acta Petrologica Sinica, 33(12): 3989～3998. (in Chinese with English abstract).

Cao Yong. 2018. Paleomagnetic constrains on the convergence and collision process of the Qiangtang and Lhasa blocks in the Tibeten Plateau. Ph. D. Dissertation. Beijing: China University of Geosciences. (in Chinese with English abstract).

Cao Yong, Sun Zhiming, Li Haibing, Pei Junling, Liu Dongliang, Zhang Lei, Ye Xiaozhou, Zheng Yong, He Xiangli, Ge Chenglong, Jiang Wang. 2019. New Paleomagnetic ResultsFrom Middle Jurassic Limestones of the Qiangtang Terrane, Tibet: Constraints on the Evolution of the Bangong-Nujiang Ocean. Tectonics, 38: 215～232.

Chang Qingsong, Zhu Dicheng, Zhao Zhidan, Dong Guochen, Mo Xuanxue, Liu Yongsheng, Hu Zhaochu. 2011. Zircon U-Pb geochronology and Hf isotopes of the Early Cretaceous Rena-Co rhyolites from southern margin of Qiangtang, Tibet, and their implications. Acta Petrologica Sinica, 27(7): 2034～2044. (in Chinese with English abstract).

Chen Weiwei, Yang Tianshui, Zhang Shihong, Yang Zhenyu, Li Haiyan, Wu Huaichun, Zhang Junhong, Ma Yiming, Cai Fulong. 2012. Paleomagnetic results from the early cretaceous zenong group volcanic rocks, Cuoqin, Tibet, and their paleogeographic implications. Gondwana Research, 22: 461～469.

Chen Weiwei, Zhang Shihong, Ding Jikai, Zhang Junhong, Zhao Xixi, Zhu Lidong, Yang Weiguang, Yang Tianshui, Li Haiyan, Wu Huaichun. 2017. Combined paleomagnetic and geochronological study on Cretaceous strata of the Qiangtang terrane, central Tibet. Gondwana Research, 41: 93～109.

Chen Weiyan, Hu Xiucheng, Zhong Yun, Fu Yuanbin, Li Fang, Wang Yuguang. 2018. Comment on "Sedimentary and Tectonic Evolution of the Southern Qiangtang Basin: Implications for the Lhasa-Qiangtang Collision Timing" by A. Ma et al. Journal of Geophysical Research: Solid Earth, 123: 7338～7342.

Cheng Xin, Wu Hanning, Diao Zongbao, Wang Haijun, Zhang XIaodong, Ma Lun, Zhou Yanan, Kang Weiwei, Ji Wenhua, Li Rongshe, Chen Shoujian, Zhao Zhenming. 2012. New paleomagnetic result of the Middle-Late Jurassic rocks from northern Qiangtang block, west China. Chinese Journal of Geophysics, 55(10): 3399～3409. (in Chinese with English abstract).

Dewey J F, Shackleton R M, Chang C F, Sun Y. 1988. The tectonic evolution of the Tibetan Plateau. Philosophical Transactions of the Royal Society of LondonA Mathematical Physical and Engineering Sciences, 327(1594): 379～413.

Fan Jianjun, Li Cai, Wang Ming, Xie Chaoming. 2018. Reconstructing in space and time the closure of the middle and western segments of the Bangong-Nujiang Tethyan Ocean in the Tibetan Plateau. International Journal of Earth Sciences, 107: 231～249.

Fan Jianjun, Li Cai, Xie Chaoming, Wang Ming, Chen Jingwen. 2015. The evolution of the Bangong-Nujiang Neo-Tethys ocean: Evidence from zircon U-Pb and Lu-Hf isotopic analyses of Early Cretaceous oceanic islands and ophiolites. Tectonophysics, 655: 27～40.

Fan Jianjun, Li Cai, Xie Chaoming, Wang Ming. 2014. Petrology, geochemistry, and geochronology of the Zhonggang ocean island, northern Tibet: implications for the evolution of the Banggongco-Nujiang oceanic arm of the Neo-Tethys. International Geology Review, 56(12): 1504～1520.

Fisher R. 1953. Dispersion on a sphere. Proceedings of the Royal Society of London, Series A, 217: 295～305.

Gao Ke, Duo Ji, Tang Juxing, Song Yang, Liu Zhibo, Fang Xiang, Yang Huanhuan, Wang Qin, Song Junlong. 2017. Geochronology and geochemistry of cryptoexplosive breccia from the Naruo Cu (Au) deposit, Tibet. Geology in China, 44(3): 618～619. (in Chinese with English abstract).

Geological Survey of Tibet Autonomous Region. 2005. 1:250,000 scale Gaize county regional geological investigation report (I45C004001). (in Chinese without English abstract).

Halim N, Cogne J P, Chen Y, Atasiei R, Besse J, Courtillot V, Gilder S, Marcoux J, Zhao R L. 1998. New Cretaceous and Early Tertiary paleomagnetic results from Xining-Lanzhou basin, Kunlun and Qiangtang blocks, China: Implications on the geodynamic evolution of Asia. Journal of Geophysical Research, 103:21025～21045.

Huang Kainian, Opdyke N D, Li Jiguang, Peng Xingjie. 1992.

Paleomagnetism of cretaceous rocks from eastern Qiangtang terrane of Tibet. Journal of Geophysical Research, 97(B2): 1789～1799.

Huang Tongtong, Xu Jifeng, Chen Jianlin, Wu Jianbin, Zeng Yunchuan. 2017. Sedimentary record of Jurassic northward subduction of the Bangong-Nujiang Ocean: insights from detrital zircons. International Geology Review, 59(2): 166～184.

Huang Wentao, Lippert P C, Zhang Yang, Jackson M J, Dekkers M J, Li Juan, Hu Xiumian, Zhang Bo, Guo Zhaojie, van Hinsbergen D J J. 2017a. Remagnetization of carbonate rocks in southern Tibet: Perspectives from rock magnetic and petrographic investigations. Journal of Geophysical Research: Solid Earth, 122, 2434～2456.

Huang Wentao, Lippert PC,Jackson M J,Zhang Yang,Li Juan,Guo Zhaojie, Kapp P, van Hinsbergen D J J. 2017b. Remagnetization of the Paleogene Tibetan Himalayan carbonate rocks in the Gamba area: Implications for reconstructing the lower plate in the India-Asia collision. Journal of Geophysical Research: Solid Earth,122: 808～825.

Huang Wentao, Jackson M J, Dekkers M J, ZhangYang,Zhang Bo, Guo Zhaojie, Dupont-Nivet G. 2019. Challenges in isolating primary remanent magnetization from Tethyan carbonate rocks on the Tibetan Plateau: Insight from remagnetized Upper Triassic limestones in the eastern Qiangtang block. Earth and Planetary Science Letters, 523: 115695.

Kapp P, DeCelles P G, Gehrels G E, Heizler M, Ding L. 2007. Geological records of the Lhasa-Qiangtang and Indo-Asian collisions in the Nima area of central Tibet. Geological Society of America Bulletin, 119: 917～933.

Kapp P, Yin A, Harrison T M, Ding L. 2005. Cretaceous-Tertiary shortening, basin development, and volcanism in central Tibet. Geological Society of America Bulletin, 117(7): 865～878.

Kirschvink J L. 1980. The Least-Squares line and plane and the analysis of paleomagnetic data. Geophysical Journal of the Royal Astronomical Society, 62: 699～718.

Lei Chuanyang, Tang Juxing, Wu Jianliang, Yin Xianke, Liu Wen, Wang Bo, Li Wei, Yuan Huayun, Zhang Wei, Yin Tao, Pei Yalun. 2019. Petro-tectonics of the volcanic rocks from the Shamuluo Fomation in Anglonggangri area located in the west segment of Bangongco-Nujiang river suture zone, Xizang (Tibet). Geological Review, 65(3): 573～588. (in Chinese with English abstract).

Li Cai, Zhai Gangyi, Wang Liquan, Yin Fuguang, Mao Xiaochang. 2009. An important window for understanding the Qinghai - Tibet Plateau—A review on research progress in recent years of Qingtang area, Tibet. China. Geological Bulletin of China, 28: 1169～1177. (in Chinese with English abstract).

Li Cai, Zhai Qingguo, Dong Yongsheng, Jiang Guangwu, Xie Chaoming, Wu Yanwang, Wang Ming. 2008. Oceanic crust on the northern margin of Gondwana—evidence from Early Paleozoic ophiolite in central Qiangtang, Qinghai-Tibet Plateau. Geological Bulletin of China, 27(10): 29～36. (in Chinese with English abstract).

Li Cai. 1987. The Longmucuo-Shuanghu-Lancangjiang plate suture and the north boundary of distribution of Gondwana facies Permo-Carboniferous system in northern Xizang, China. Journal of Changchun College of Geologu, 17(2): 155～166. (in Chinese with English abstract).

Li Shun, Guilmette C, Ding Lin, Xu Qiang, Fu Jiajun, Yue Yahui. 2017. Provenance of Mesozoic clastic rocks within the Bangong-Nujiang suture zone, central Tibet: Implications for the age of the initial Lhasa-Qiangtang collision. Journal of Asian Earth Sciences, 147: 469～484.

Li Yalin, He Juan, Wang Chengshan, Han Zhongpeng, Ma Pengfei, Xu Ming, Du Kaiyuan. 2015. Cretaceous volcanic rocks in south Qiangtang Terrane: Products of northward subduction of the Bangong-Nujiang Ocean? Journal of Asian Earth Sciences, 104: 69～83.

Li Yalin, He Juan, Wang Chengshan, Santosh M, Dai Jingen, Zhang Yuxiu, Wei Yushuai, Wang Jiangang. 2013. Late Cretaceous K-rich magmatism in central Tibet: Evidence for early elevation of the Tibetan plateau? Lithos, 160～161: 1～13.

Liu Deliang, Huang Qishuai, Fan Shuaiquan, Zhang Liyuan, Shi Rendeng, Ding Lin. 2014. Subductionof the Bangong-Nujiang Ocean: constraints from granites in the Bangong Co area, Tibet. Geological Journal, 49(2): 188～206.

Liu Hong, Li Guangming, Huang Hanxiao, Zhang Zhilin, Xiao Wanfeng, Jiao Yanjie, Liang Shengxian, Guo Jin, Lan Shuangshuang. 2017. Prospecting potential analysis of deep No. Ⅲ ore section in the Shangxu orogenic gold deposit, Bangong Co-Nujiang metallogenic Belt, Tibet. Acta Geologica Sinica, 91(6): 1245～1258. (in Chinese with English abstract).

Liu Weiliang, Xia Bin, Zhong Yun, Cai Jianxin, Li Jianfeng, Liu Hongfei, Cai Zhourong, Sun Zhilei. 2014. Age and composition of the Rebang Co and Julu ophiolites, central Tibet: implications for the evolution of the Bangong Meso-Tethys. International Geology Review, 56(4): 430～447.

Ma Aanlin and Hu Xiumian. 2018. Reply to Comment by W. Y. Chen et al. on "Sedimentary and Tectonic Evolution of the Southern Qiangtang Basin: Implications for the Lhasa-Qiangtang Collision Timing". Journal of Geophysical Research: Solid Earth, 123: 7343～7346.

Ma Aanlin, Hu Xiumian, Garzanti E, Han Zhong, Lai Wen. 2017. Sedimentary and tectonic evolution of the southern Qiangtang basin: Implications for the Lhasa Qiangtang collision timing. Journal of Geophysical Research: Solid Earth, 122: 4790～4813.

Ma Yiming, Wang Qiang, Wang Jun, Yang Tianshui, Tan Xiaodong, Dan Wei, Zhang Xiuzheng, Ma Lin, Wang Ziliang, Hu Wanlong, Zhang Shihong, Wu Huaichun, Li Haiyan, Cao Liwan. 2019. Paleomagnetic Constraints on the Origin and Drift History of the North Qiangtang Terrane in the Late Paleozoic. Geophysical Research Letters, 46: 689～697.

Ma Yiming, Yang Tianshui, Bian Weiwei, Jin Jingjie, Wang Qiang, Zhang Shihong, Wu Huaichun, Li Haiyan, Cao Liwan. 2018. A stable southern margin of Asia during the Cretaceous: paleomagnetic constraints on the Lhasa-Qiangtang collision and the maximum width of the Neo-Tethys. Tectonics, 37(10): 3853～3876.

Ma Yiming, Yang Tianshui, Bian Weiwei, Jin Jingjie, Wang Qiang, Zhang Shihong, Wu Huaichun, Li Haiyan, Cao Liwan, Yuan Haifan, Ding Jikai. 2017. Paleomagnetic and geochronologic results of latest Cretaceous lava flows from the Lhasa Terrane and their tectonic implications. Geophysical Research: Solid Earth, 122: 8786～8809.

Ma Yiming, Yang Tianshui, Yang Zhenyu, Zhang Shihong, Wu Huaichun, Li Haiyan, Li Huaikun, Chen Weiwei, Zhang Junhong, Ding Jikai. 2014. Paleomagnetism and U-Pb zircon geochronology of Lower Cretaceous lava flows from the western Lhasa terrane: new constraints on the India-Asia collision process and intracontinental deformation within Asia. Journal of Geophysical Research: Solid Earth, 119: 7404～7424.

McFadden P L. 1990. A new fold test for paleomagnetic studies. Geophysics journal International, 103: 163～169.

Meng Jun, Zhao Xixi, Wang Chengshan, Liu Hao, Li Yalin, Han Zhongpeng, Liu Tao, Wang Meng. 2018. Palaeomagnetism and detrital zircon U-Pb geochronology of Cretaceous redbeds from central Tibet and tectonic implications. Geological Journal, 53(5): 2315～2333.

Metcalfe I. 2006. Palaeozoic and Mesozoic tectonic evolution and palaeogeography of East Asian crustal fragments: The Korean Peninsula in context. Gondwana Research, 9: 24～46.

Metcalfe I. 2013. Gondwana dispersion and Asian accretion: Tectonic and palaeogeographic evolution of eastern Tethys. Journal of Asian Earth Sciences, 66: 1～33.

Mo Xuanxue and Pan Guitang. From the Tethys to the formation of the Qinghai -Tibet Plateau: constrained by tectono-magmatic events. Earth Science Frontiers, 13(6): 43～51. (in Chinese with English abstract).

Murphy M A, Yin A, Harrision T M, Durr S B, Chen Z, Ryerson F J, Kidd W S F, Wang X, Zhou X. 1997. Did the Indo-Asian collision alone create the Tibetan plateau? Geology, 25(8): 719～722.

Peng Touping, Zhao Guochun, Fan Weiming, Peng Bingxia, Mao Yongsheng. 2015. Late Triassic granitic magmatism in the Eastern Qiangtang, Eastern Tibetan Plateau: Geochronology, petrogenesis and implications for the tectonic evolution of the Paleo-Tethys. Gondwana Research, 27: 1494～1508.

Ran Bo, Deng Bin, Wang Chengshan, Zhao Xixi, Li Yalin, Zhang Yuxiu, Meng Jun, He Meng, Zhu Lidong, Christopher X. 2017. Kinematics of the crust around the Tanggula Shan in North-Central Tibet: Constraints from paleomagnetic data. Gondwana Research, 48: 124～133.

Ren Haidong, Yan Maodu, Meng Qingquan, Song Chunhui, Fang Xiaomin. 2013. "E/I" corrected paleomagnetic inclination indicates 1000 km N-S shorting of the Qiangtang terrane since the Middle Jurassic. Chinese Journal of Geology, 48(2): 543～556. (in Chinese with English abstract).

Sengör A M C. 1987. Tectonics of the Tethysides: Orogenic Collage Development in a Collisional Setting. Annual Review of Earth and Planetary Sciences, 15: 213～244.

Song Chunyan, Wang Jian, Fu Xiugen, Feng Xinglei, Chen Ming, He Li. 2012. Late Triassic paleomagnetic data from the Qiangtang terrane of Tibetan Plateau and their tectonic significances. Journal of Jilin University (Earth Science Edition), 42(2):241～250. (in Chinese with English abstract).

Song Peiping, Ding Lin, Li Zhenyu, Lippert P C, Yang Tianshui, Zhao Xixi, Fu Jiajun, Yue Yahui. 2015. Late Triassic paleolatitude of the Qiangtang block: Implications for the closure of the Paleo-Tethys Ocean. Earth and Planetary Science Letters, 424: 69～83.

Song Peiping, Ding Lin, Li Zhenyu, Lippert P C, Yue Yahui. 2017. An early bird from Gondwana: Paleomagnetism of Lower Permian lavas from northern Qiangtang (Tibet) and the geography of the Paleo-Tethys. Earth and Planetary Science Letters, 475: 119～133.

Song Yang, Tang Juxing, Qu Xiaoming, Wang Denghong, Xin Hongbo, Yang Chao, Lin Bin, Fan Shufang. 2014. Progress in the study of mineralization in the Bangongco-Nujiang metallogenic belt and some new recognition. Advances in Earth Science, 29(7): 795～809. (in Chinese with English abstract).

Sun Gaoyuan, Hu Xiumian, Xu Yiwei, BouDagher-Fadel M K. 2019. Discovery of Middle Jurassic trench deposits in the Bangong-Nujiang suture zone: Implications for the timing of Lhasa-Qiangtang initial collision. Tectonophysics, 750: 344～358.

Tang Juxing, Wang Qin, Yang Huanhuan, Gao Xin, Zhang Zebin, Zou Bing. 2017. Mineralization, Exploration and Resource Potential of Porphyry-skarn-epithermal Copper Polymetallic Deposits in Tibet. Acta Geoscientica Sinica, 38(5): 571～614. (in Chinese with English abstract).

Tang Xiangde, Huang Baochun, Yang Liekun, Yi Zhiyu, Qiao Qingqing, Chen Liwei. 2013. Paleomagnetism and Ar-Ar geochronology of Cretaceous volcanic rocks in the middle Lhasa terrane, China and tectonic implications. Chinese Journal of Geophysics, 56: 136～149. (in Chinese with English abstract).

Tauxe L and Kent D V. 2004. A simplified statistical model for the geomagnetic field and the detection of shallow bias in paleomagnetic inclinations: was the ancient magnetic field dipolar? Geophysical Monograph, 145:101～115.

Tong Yabo, Yang Zhenyu, Gao Liang, Wang Heng, Zhang Xudong, An Chunzhi, Xu Yingchao, Han Zhirui. 2015. Paleomagnetism of Upper Cretaceous red-beds from the eastern Qiangtang Block: Clockwise rotations and latitudinal translation during the India-Asia collision. Journal of Asian Earth Sciences, 114: 732～749.

Tong Yabo, Yang Zhenyu, Mao Changping, Pei Junling, Pu Zongwen, Xu Yingchao. 2017. Paleomagnetism of Eocene red-beds in the eastern part of the Qiangtang Terrane and its implications for uplift and southward crustal extrusion in the southeastern edge of the Tibetan Plateau. Earth and Planetary Science Letters, 475: 1～14.

Van der Voo R. 1990. The reliability of paleomagnetic data. Tectonophysics, 184: 1～9.

Volkmer J E, Kapp P, Guynn J H, Lai Qingzhou. 2007. Cretaceous-Tertiary structural evolution of thenorth central Lhasa terrane, Tibet. Tectonics, 26: TC6007.

Volkmer J E, Kapp P, Horton B K, Gehrels G E, Minervini J M, Ding L. 2014. Northern Lhasa thrust belt of central Tibet: Evidence of Cretaceous-early Cenozoic shortening within a passive roof thrust system? in Nie J, Horton BK, and Hoke GD, eds., Toward an Improved Understanding of Uplift Mechanisms and the Elevation History of the Tibetan Plateau: Geological Society of America, 59～70.

Wang Baodi, Wang Liquan, Chung Sunlin, Chen Jianlin, Yin Fuguang, Liu Han, Li Xiaobo, Chen Lingkang. 2016. Evolution of the Bangong-Nujiang Tethyan ocean: Insights from the geochronology and geochemistry of mafic rocks within ophiolites. Lithos, 245: 18～33.

Wang Chengshan, Dai Jingen, Zhao Xixi, Li Yalin, Graham S A, He Dengfa, Ran Bo, Meng Jun. 2014. Outward-growth of the Tibetan Plateau during the Cenozoic: A review. Tectonophysics, 621: 1～43.

Watson G S and Enkin R J. 1993. The fold test in paleomagnetism as a parameter estimation problem. Geophysics Research Letter, 20: 2135～2137.

Xu Mengjing, Li Cai, Xu Wei, Xie Chaoming, Hu Peiyuan, Wang Ming. 2014. Petrology, Geochemistry and Geochronology of Gabbros from the Zhongcang Ophiolitic Mélange, Central Tibet: Implications for an Intra-Oceanic Subduction Zone within the Neo-Tethys Ocean. Journal of Earth Science 25, 224～240.

Xu Ronghua, Schärer U, Allègre C J. 1985. Magmatism and metamorphism in the Lhasa block (Tibet): a geochronological study. The Journal of Geology, 93(1): 41～57.

Xu Wei, Li Cai, Xu Mengjing, Wu Yanwang, Fan Jianjun, Wu Hao. 2015. Petrology, geochemistry, and geochronology of boninitic dikes from the Kangqiong ophiolite: implications for the Early Cretaceous evolution of Bangong-Nujiang Neo-Tethys Ocean in Tibet. International Geology Review, 57:2028～2043.

Xu Zhiqin, Yang Jingsui, Li Haibing, Zhang Zeming, Liu Yan. 2011. On the tectonics of the India-Asia Collision. Acta Geologica Sinica, 85(1): 1～33. (in Chinese with English abstract).

Xu Zhiqin, Yang Jingsui, Li Wenchang, Li Huaqi, Cai Zhihui, Yan Zhen, Ma Changqian. 2013. Paleo-Tethys system and accretionary orogen in the Tbiet Plateau. Acta Petrologica Sinica, 29(6): 1847～1860. (in Chinese with English abstract).

Xu Zhiqin, Zhao Zhongbao, Peng Miao, Ma Xuxuan, Li Huaqi, Zhao Junmeng. 2016. Review of "orogenic plateau". Acta Petrologica Sinica, 32(12): 3557～3571. (in Chinese with English abstract).

Yan Maodu, Zhang Dawen, Fang Xiaomin, Ren Haidong, Zhang Weilin, Zan Jinbo, Song Chunhui, Zhang Tao. 2016. Paleomagnetic data bearing on the Mesozoic deformation of the Qiangtang Block: Implications for the evolution of the Paleo- and Meso-Tethys. Gondwana Research, 39: 292～316.

Yang Tianshui, Ma Yiming, Zhang Shihong, Bian Weiwei, Yang Zhenyu, Wu Huaichun, Li Haiyan, Chen Weiwei, Ding Jikai. 2015. New insights into the India-Asia collision process from Cretaceous paleomagnetic and geochronologic results in the Lhasa terrane. Gondwana Research, 28: 625～641.

Yi Zhiyu, Huang Baochun, Yang Liekun, Tang Xiangde, Yan Yonggang, Qiao Qingqing, Zhao Jie, Chen Liwei. 2015. A quasi-linear structure of the southern margin of Eurasia prior to the India-Asia collision: First paleomagnetic constraints from Upper Cretaceous volcanic rocks near the western syntaxis of Tibet. Tectonics, 34(7): 1431～1451.

Yin A and Harrison T M. 2000. Geologic evolution of the Himalayan-Tibetan orogen. Annual Review of Earth and Planetary Sciences, 28: 211～280.

Zhang Kaijun, Xia Bin, Zhang Yuxiu, Liu Weiliang, Zeng Lu, Li Jianfeng, Xu Lifeng. 2014. Central Tibetan Meso-Tethyan oceanic plateau. Lithos, 210～211: 278～288.

Zhang Kaijun, Zhang Yuxiu, Tang Xianchun, Xia Bin. 2012. Late Mesozoic tectonic evolution and growth of the Tibetan plateau prior to the Indo-Asian collision. Earth-Science Reviews, 114: 236～249.

Zheng Youye, Ci Qiong, Wu Song, Jin Liangxu, Guo Jianci, Ci Renji, Gong Fuzhi, Tan Meng, Zhang Hongqiang. 2017. The discovery and significance of Rongga porphyry Mo deposit in the Bangong-Nujiang metallogenic belt, Tibet. Earth Science, 42(9): 1441～1453. (in Chinese with English abstract).

Zhu Dicheng, Li Shimin, Cawood P A, Wang Qing, Zhao Zhidan, Liu Shengao, Wang Liquan. 2016. Assembly of the Lhasa and Qiangtang terranes in central Tibet by divergent double subduction. Lithos, 245: 7～17.

Zhu Dicheng, Zhao Zhidan, Niu Yaoling, Dilek Y, Hou Zengqian, Mo Xuanxue. 2013. The origin and pre-Cenozoic evolution of the Tibetan Plateau. Gondwana Research, 23: 1429～1454.

参考文献

毕志伟，李志敏，李强，王艳凯，孙肖，张涛. 2018. 羌塘地块西南缘上侏罗统—下白垩统海相地层的发现. 沉积与特提斯地质，38(1): 1～10.

曹勇，孙知明，刘栋梁，张蕾，叶小舟，郑勇，何祥丽. 2017. 拉萨地块北缘尼玛地区晚白垩世古地磁结果及其构造意义. 岩石学报，33(12): 3989～3998.

曹勇. 2018. 青藏高原羌塘地块与拉萨地块汇聚—碰撞过程的古地磁制约. 博士学位论文. 北京：中国地质大学.

常青松，朱弟成，赵志丹，董国臣，莫宣学，刘勇胜，胡兆初. 2011. 西藏羌塘南缘热那错早白垩世流纹岩锆石 U-Pb 年代学和 Hf 同位素及其意义. 岩石学报，27(7): 2034～2044.

程鑫，吴汉宁，刁宗宝，王海军，张晓东，马轮，周亚楠，康伟伟，计文化，李荣社，陈守建，赵振明. 2012. 羌北地块中—晚侏罗世雁石坪群古地磁新结果. 地球物理学报，55(10): 3399～3409.

高轲，多吉，唐菊兴，宋扬，刘治博，方向，杨欢欢，王勤，宋俊龙. 2017. 西藏拿若铜(金)矿床隐爆角砾岩锆石 U-Pb 年代学及地球化学特征. 中国地质，44(3): 618～619.

雷传扬，唐菊兴，吴建亮，尹显科，刘文，王波，李威，袁华云，张伟，尹滔，裴亚伦. 2019. 班公湖—怒江缝合带西段昂龙岗日地区沙木罗组火山岩的岩石大地构造学研究. 地质论评，65(3): 573～588.

李才，翟刚毅，王立全，尹福光，毛晓长. 2009. 认识青藏高原的重要窗口——羌塘地区近年来研究进展评述(代序). 地质通报，28(9): 1169～1177.

李才，翟庆国，董永胜，蒋光武，解超明，吴彦旺，王明. 2008. 冈瓦纳大陆北缘早期的洋壳信息——来自青藏高原羌塘中部早古生代蛇绿岩的依据. 地质通报，27(10): 29～36.

李才. 1987. 龙木错—双湖—澜沧江板块缝合带与石炭二叠纪冈瓦纳北界. 吉林大学学报：地球科学版，17(2): 155～166.

刘洪，李光明，黄瀚霄，张智林，肖万峰，焦彦杰，梁生贤，郭境，兰双双. 2017. 班公湖—怒江成矿带商旭造山型金矿床Ⅲ号矿段深部找矿潜力研究. 地质学报，91(6): 1245～1258.

莫宣学和潘桂棠. 2006. 从特提斯到青藏高原形成：构造—岩浆事件的约束. 地学前缘，13(6): 43～51.

任海东，颜茂都，孟庆泉，宋春晖，方小敏. 2013. 羌塘盆地磁倾角浅化校正及其在构造上的应用—中侏罗纪以来约 1000km 的南北向缩短. 地质科学，48(2): 543～556.

宋春彦，王剑，付修根，冯兴雷，陈明，何利. 2012. 青藏高原羌塘盆地晚三叠世古地磁数据及其构造意义. 吉林大学学报(地球科学版)，42(2): 241～250.

宋扬，唐菊兴，曲晓明，王登红，辛洪波，杨超，林彬，范淑芳. 2014. 西藏班公湖—怒江成矿带研究进展及一些新认识. 地球科学进展，29(7): 795～809.

唐菊兴，王勤，杨欢欢，高昕，张泽斌，邹兵. 2017. 西藏斑岩—矽卡岩—浅成低温热液铜多金属矿成矿作用、勘查方向与资源潜力. 地球学报，38(5): 571～614.

唐祥德，黄宝春，杨列坤，易治宇，乔庆庆，陈力为. 2013. 拉萨地块中部晚白垩世火山岩 Ar-Ar 年代学和古地磁研究结果及其构造意义. 地球物理学报，56(1): 136～149.

西藏自治区地质调查院. 2006. 中华人民共和国区域地质调查报告(1：250000)改则县幅(I45C004001).

许志琴，杨经绥，李海兵，嵇少丞，张泽明，刘焰. 2011. 印度—亚洲碰撞大地构造. 地质学报，85(1): 1～33.

许志琴，杨经绥，李文昌，李化启，蔡志慧，闫臻，马昌前. 2013. 青藏高原中的古特提斯体制与增生造山作用. 岩石学报，29(6): 1847～1860.

许志琴，赵中宝，彭淼，马绪宣，李化启，赵俊猛. 2016. 论“造山的高原”. 岩石学报，32(12): 3557～3571.

郑有业，次琼，吴松，晋良旭，郭建慈，次仁吉，龚福志，谭勐，张弘强. 2017. 西藏班公湖—怒江成矿带荣嘎斑岩型钼矿床的发现及意义. 地球科学，42(9): 1441～1453.

Paleomagnetic study of the Late Triassic limestones in the western portion of the Qiangtang Block and its tectonic implications

CAO Yong[1,2], SUN Zhiming[1], LI Haibing[2], YE Xiaozhou[1],
PAN Jiawei[2], ZHANG Lei[2], LIU Dongliang[2], LIU Chenguang[1]

1) *MNR Key Laboratory of Paleomagnetism and Tectonic Reconstruction, Institute of Geomechanics, Chinese Academy of Geological Sciences, Beijing*, 100081;

2) *MNR Key Laboratory of Deep-Earth Dynamics, Institute of Geology, Chinese Academy of Geological Sciences, Beijing*, 100037

* *Corresponding author: geocao@126.com*

Abstract

The processes of the collision between the Qiangtang and Lhasa blocks is a key factor to understanding the evolution history and geodynamics of the central Tibetan Plateau. The paleomagnetic study for the Qiangtang block is critical to understand these questions. A paleomagnetic study of the Late Triassic limestones from the Gaize area in the western portion of the Qiangtang block has been carried out and a remagnetization component has been obtained. The mean direction of the characteristic remanent component in geographic coordinates is $Dg=349.3°$, $Ig=40.4°$, $\kappa g=45.4$, $\alpha_{95}=6.5°$, corresponding to a paleopole at 76.4 °N, 311.1 °E with $dp/dm=4.7°/7.9°$. This pole coincides with the Early Cretaceous (ca. 110～100 Ma) paleomagnetic pole of the Qiangtang block, indicating the age of the remagnetization is 110～100 Ma. Our new results, combined with previous reliable Cretaceous paleomagnetic results from the Qiangtang and Lhasa blocks and synthesize stratigraphy, ophiolite and ocean island evidence, suggested that the final closure of western portion of the Bangong-Nujiang Tethys Ocean may have occurred during 110～100 Ma. Furthermore, the late Early Cretaceous remagnetization of the Late Triassic limestones in the Gaize area was closely related with the Qiangtang-Lhasa collision.

Key words: Qiangtangblock; paleomagnetism; remagnetization; Qiangtang-Lhasa collision; Bangong-Nujiang Ocean